

MVSA-Net: Multi-View State-Action Recognition for Robust and Deployable Trajectory Generation

Ehsan Asali, Prashant Doshi, Jin Sun¹

Abstract—The learn-from-observation (LfO) paradigm is a human-inspired mode for a robot to learn to perform a task simply by watching it being performed. LfO can facilitate robot integration on factory floors by minimizing disruption and reducing tedious programming. A key component of the LfO pipeline is a transformation of the depth camera frames to the corresponding task state and action pairs, which are then relayed to learning techniques such as imitation or inverse reinforcement learning for understanding the task parameters. While several existing computer vision models analyze videos for activity recognition, SA-Net specifically targets robotic LfO from RGB-D data. However, SA-Net and many other models analyze frame data captured from a single viewpoint. Their analysis is therefore highly sensitive to occlusions of the observed task, which are frequent in deployments. An obvious way of reducing occlusions is to simultaneously observe the task from multiple viewpoints and synchronously fuse the multiple streams in the model. Toward this, we present multi-view SA-Net, which generalizes the SA-Net model to allow the perception of multiple viewpoints of the task activity, integrate them, and better recognize the state and action in each frame. Performance evaluations on two distinct domains establish that MVSA-Net recognizes the state-action pairs under occlusion more accurately compared to single-view MVSA-Net and other baselines. Our ablation studies further evaluate its performance under different ambient conditions and establish the contribution of the architecture components. As such, MVSA-Net offers a significantly more robust and deployable state-action trajectory generation compared to previous methods.

I. INTRODUCTION

Learn-from-observation (LfO) is the human-inspired methodology of observing an expert (usually a human) performing a task and learning a computational representation of the behavior that can then be used by a robotic agent to perform the task as well as the expert [2], [3]. In most methods that enable LfO, the agent learns a mapping between the states of the environment and available actions. This mapping is known as a policy, which the agent later uses to perform the task in the environment. Instead of directly training an end-to-end policy for predicting low-level robotic actions, our approach involves the classification of high-level state-action samples extracted from sensor streams. The main motivation for such a learning paradigm arises from the learner’s objective, which may not only be to replicate the expert’s actions but also to comprehend the expert’s preferences. This comprehension is achieved through the learning of a reward function using state-of-the-art inverse RL methodologies, which, in turn, aids in task acquisition. Consequently, the

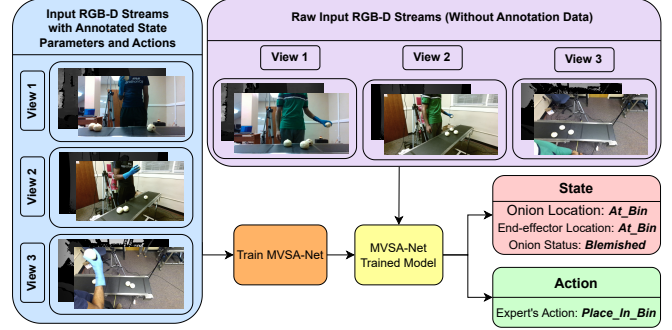


Fig. 1: An overview of how to use MVSA-Net for trajectory generation in a custom domain (onion-sorting) having three input RGB-D streams. First, synchronized RGB-D frames are annotated and used to train the state and action classifiers. Later, unseen synchronized RGB-D frames can be fed to the trained MVSA-Net model to predict the state parameters and the expert’s action. In the above example, the expert is about to place a blemished onion in a cardboard box (bin) which is located behind the conveyor belt.

learner becomes adaptable to novel scenarios, as it has gleaned the expert’s preferences instead of just adhering to a rigid policy.

In order to bridge the gap between the raw vision (often RGB-D) sensor stream input and the state-action samples as specified by the environment model, several previous computer vision models exist that analyze videos for activity recognition [1], [16], and there are analogous ones for robots that analyze depth camera streams [10], [11], [12]. A particular deep neural network model specifically aimed for robotic LfO from RGB-D data is SA-Net [27]. A trained SA-Net model processes raw RGB-D streams from a single depth camera and produces joint state-action trajectories. SA-Net’s convolutional layers utilize the RGB channels to extract spatial information and identify the state, while time-distributed CNNs and LSTMs [14] handle action recognition. To recognize actions, the network extracts spatial and temporal information to predict motion direction. Nonetheless, this limitation to a single viewpoint comes with well-known challenges. A perception sensor’s field of view (FoV) determines the span of its visibility, limiting the information it gathers. Sensor streams exhibit various levels of hardware noise, characterized by their signal-to-noise ratio.

Finally, unavoidable occlusions in the environment could block the view of the camera. To illustrate this, consider the use case of LfO of a human sorting produce on a conveyor in a farm-based packing shed. The wall-mounted depth camera sensor may get irregularly obstructed by other line workers,

¹Ehsan Asali, Prashant Doshi, and Jin Sun are with the School of Computing, University of Georgia, Athens GA 30606, USA ehsanasali@uga.edu

humans wishing to converse with the observed human, or small vehicles moving about on the shed floor [7], [29]. LfO paradigms and specifically IRL techniques are highly susceptible to occlusion and noise, while these challenges are common in deployed environments. Our multi-view model is best suited in such cases where the chance of occlusion and/or noise is high or when the domain is sensitive and losing track of states/actions can harm the system significantly. Furthermore, a single sensor is insufficient to capture both the actions and what the human sees as it inspects the produce.

In this paper, we present MVSA-Net, a model that enables input from multiple viewpoints and recognizes state-action pairs from multiple synchronized RGB-D data streams. MVSA-Net is a generalized model that leverages multiple heterogeneous visual sensors to simultaneously identify the expert’s states and actions in challenging real-world scenarios. For our produce processing use case, multiple depth cameras can allow both the expert’s actions and his or her view of the product during inspection to be recorded; multiple viewpoints also help mitigate the detrimental effects of occlusions and sensor noise on LfO. MVSA-Net utilizes gating networks [9] to establish a mixture-of-experts layer, where several expert models represented by input streams make classification choices and gating controls how to weigh the classifications in a probabilistic input-dependent manner. Thus, the gating dynamically distributes the decision-making to the different views for optimal performance. The model employs time-distributed CNNs and GRU recurrent units, receiving frames from the current time step t and the four previous time steps to create a temporal context that facilitates action recognition.

We conduct a comprehensive performance evaluation of MVSA-Net in two robotic domains. In the first domain, we illustrate the produce-sorting task, where a human expert sorts onions, retaining unblemished onions on the conveyor while removing blemished ones upon inspection. In this scenario, the model processes three RGB-D camera streams concurrently to identify the state, including the onion’s location, the end-effector’s (sorter’s hand) position, the onion status, and the expert’s actions. We employ a custom-trained YOLOv5 instance [24] to classify the onion. The second domain involves mobile robot patrolling, as introduced in [6], where two TurtleBots patrol a hallway simultaneously but independently. Another TurtleBot observes the patrollers from a vantage point and attempts to penetrate the patrol. To assist the attacker, we install an additional camera at a second vantage point in our experiments. The attacker utilizes MVSA-Net to recognize patrollers’ movements. In both domains, MVSA-Net demonstrates a significant improvement in state-action prediction accuracy when compared to single-view and multi-view baselines. Furthermore, our comprehensive ablation studies validate MVSA-Net’s effectiveness and robustness in challenging scenarios, such as malfunctioning sensors and varying lighting conditions. These ablation studies also empirically establish the necessity of specific modules in the model’s architecture. MVSA-Net is, to our knowledge, the first model for multiple viewpoint state-action pair recognition, facilitating robot LfO.

II. RELATED WORK

Recent advances enabled by deep neural networks have significantly enhanced the performance of image and video classification tasks [13], [35]. A substantial body of work has predominantly concentrated on single-view human activity and action recognition [25], [33], [27]. Although these techniques excel under normal conditions, they are susceptible to environmental occlusions and sensor noise in the data.

Multi-modal and multi-view sensor input in the context of classification problems has been shown to overcome the limitations of single-view or single-modality systems. For instance, Asali et al. [5] utilize visual and audio streams within a deep multi-modal architecture to conduct speaker recognition in video clips. Shin et al. [26] introduced a context-aware collaborative pipeline for multi-view object recognition. The pipeline extracts features from each view at each time step, applies view pooling to the aggregated result, and conducts a global prediction for each frame’s object class. Lu et al. [20] present a multi-camera pipeline that detects objects in each camera stream using shared pseudo-labels and performs a consistency learning step. Kasaei et al. [17] developed a deep learning architecture equipped with augmented memories to concurrently address open-ended object recognition and grasping. This method accepts multiple views of an object as input and jointly estimates pixel-wise grasp configurations and scale-and-rotation-invariant feature representations as outputs. Strbac et al. [28] put forward a YOLO detector model and the principles of stereoscopy to substitute the Light Detection And Ranging (LiDAR) sensors with cameras for distance estimation. In [22], Nieto et al. introduce a multi-camera people detection framework that employs a camera transference unit to transfer detection results from auxiliary cameras to the primary camera. This method can transfer detections to a different point of view, automatically combine multiple cameras, and automatically select the working threshold for each of them.

Some works investigate the utilization of multi-view [31], [19], [32] or multi-modality [21] data in action recognition tasks. For instance, Vyas et al. [31] suggest an unsupervised representation learning framework that encodes scene dynamics in videos captured from multiple viewpoints and predicts actions from unseen views using RGB data. Nevertheless, this method is susceptible to performance degradation in the presence of noise in one or multiple views. Additionally, it employs multiple views during training but only a single view during testing. In contrast, MVSA-Net learns the states and actions of a person from each viewpoint and subsequently predicts the state-action pair from multiple views. Wang et al. [32] propose a multi-branch network called DA-Net for multi-view action recognition. DA-Net exchanges messages among view-specific features from different branches and employs a view-prediction-guided fusion method to produce combined action classification scores. While these methods focus on multi-view or multi-modality object-detection or action recognition, MVSA-Net simultaneously recognizes state-action pairs for LfO tasks.

To explicitly model temporal dependencies in video frames for action recognition, a few methods have used long short-term memories (LSTMs) [30], [34]. LSTMs, as part of the recurrent neural networks (RNNs) family, extract dynamic features from videos. A more efficient and simpler RNN architecture is the gated recurrent unit (GRU). Both GRUs and LSTMs can learn dynamic video features and mitigate the vanishing gradient problem, a common issue in deep neural network training. In MVSA-Net we choose GRUs over LSTMs due to their simpler structure and faster training characteristics. Additionally, GRUs perform well with video frames where actions occur over short durations, aligning with our task setup.

III. MULTI-VIEW SA-NET

In this section, we provide a detailed description of MVSA-Net’s architecture. It effectively utilizes both convolutional and recurrent neural network modules and allows for a multitude of input streams. Its adaptable design facilitates easy customization for a wide range of application domains.

A. Method Overview

We are interested in the problem of estimating the states and actions of experts performing a task from multiple heterogeneous sensors, including RGB-D cameras. The task can be performed by one or multiple humans and/or robots, either real or simulated, who are capable of performing it optimally. We propose to use convolutional and recurrent deep neural networks to analyze the sensory streams from the heterogeneous sensors and extract spatial and temporal information. This information is then employed for recognizing the states and actions of the experts performing the task. To be specific, given n number of consecutive video frames of an expert performing a task (time steps $t, t-1, \dots, t-(n-1)$), a learner utilizes MVSA-Net to jointly predict the state and action at the current time step t . In our experiments, we set n to 5 as it helps to recover sufficient information from previous time steps to recognize the performed action with relatively high accuracy. Fig. 2 illustrates MVSA-Net configured with two cameras/views. MVSA-Net is adaptable and capable of accommodating any number of views (limited to the hardware capacity), depending on the specific application domain. We discretize the state and action spaces to formulate the learning task as a classification problem.

In a general context, each view can be either a uni-modal (i.e. either RGB or depth) or a multi-modal (RGB-D) video stream. In **state recognition**, the RGB and depth frames from the most recent time step undergo processing through a series of convolutional and pooling layers. The final pooling layer’s output is flattened into a 1-D vector and subsequently fed into a neural network known as the state classifier, comprising two hidden layers and one output layer. The state classifier network is a multi-head neural network that calculates the probability distribution for each state parameter based on the input frame (i.e., the number of head/output nodes equals the number of state parameters). The gating network combines the flattened layers from all views into a single input and

generates a probability distribution across the viewpoints. The gating network’s architecture mirrors that of the state classifier, with the key difference being that it outputs the probability of each view making a correct prediction about the states (i.e., the number of head/output nodes matches the number of viewpoints).

The **action recognition** branch follows a similar process, except that it retrieves n consecutive video frames from each video stream and employs Time Distributed (TD) convolutions and GRU layers to extract crucial temporal features. The gating network utilized for action recognition not only leverages the data from the GRU units but also integrates the aggregated information from the flattened layers of state recognition. The intuition is that the current action and state are strongly correlated. In both the state and action recognition tasks, a decision module is employed to gather the output results from each viewpoint and the gating network, ultimately generating the final output.

In the following subsections, we describe the state and action recognition mechanisms in full detail, respectively.

B. State Recognition

The network architecture for generating the state parameters is simple yet efficient. It starts by fetching the latest RGB-D frame from each view, concatenating them into a single multi-dimensional tensor, and subsequently inputting this combined data into a sequence of five convolutional layers and three pooling layers. Each convolutional layer uses 32 filters with a kernel size of 3×9 and a stride of 3×3 , with the exception of the final convolutional layer, which uses a stride of 2×2 . The pooling layers are located after the first, third, and fifth convolutional layers, respectively, with pooling sizes of 4×4 , 2×2 , and 2×2 and strides of 3×3 , 3×3 , and 2×2 , respectively. To ensure stable training, batch normalization is implemented after the fifth convolutional layer, following the methodology outlined in [15]. Since the state features are not a temporal construct and they represent spatial locations of objects as well as visual object specifications, stacking multiple observations would be redundant for state recognition.

After applying convolution, pooling, and batch normalization operations, the resulting tensor is flattened into a one-dimensional feature vector. Each feature vector (f_n) serves as input for the state classifier specific to its corresponding viewpoint (C_n). Meanwhile, the gating network takes in the aggregated feature vectors from all views (f) and generates a probability distribution across the viewpoint branches (G_n). Then, the decision module takes the weighted outputs of each classifier and performs a pairwise addition to unify the vectors. Finally, the output label (L) index is obtained by applying the argmax function to the unified vector, as demonstrated in Eq. 1.

$$L = \operatorname{argmax} \left(\sum_n G_n(f) \cdot C_n(f_n) \right) \quad (1)$$

The design of the gating network involves assigning a lower weight to the feature vector of a noisy or less informative

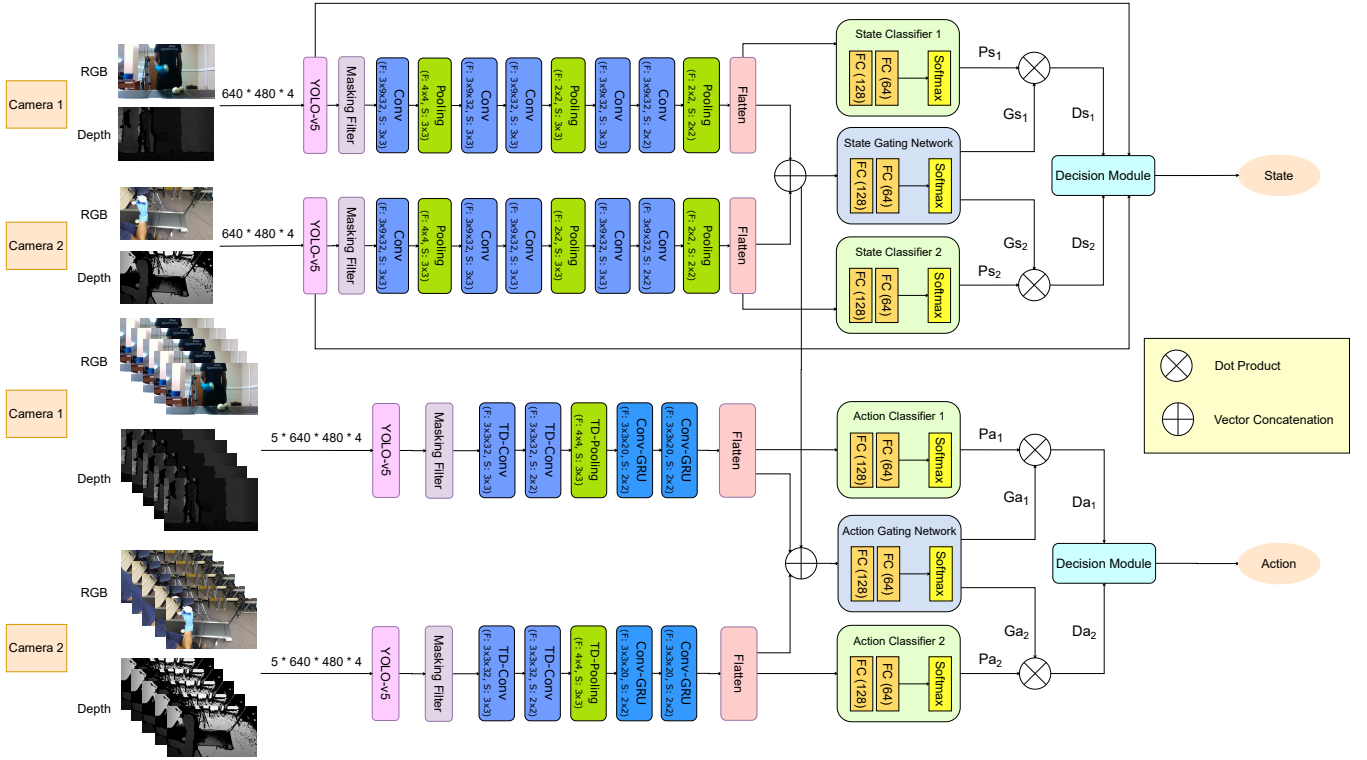


Fig. 2: An overview of the MVSA-Net architecture. The network jointly predicts the state and action of an expert using multiple heterogeneous synchronized RGB-D frames. The so-called RGB-D frames are processed through a deep convolutional and recurrent neural network, which predicts both the state labels and the expert’s actions. YOLO-v5 contributes to the network’s masking paradigm and aids the decision module in achieving more accurate state predictions. The masking paradigm functions such that when it detects more than one expert in a frame, it automatically converts the input frame into multiple frames, each containing only a single expert.

view and assigning a higher weight to the feature vector of a useful view for predicting the label. The dynamic weighting of diverse views empowers the gating network to optimize each view’s contribution and improve the effectiveness of the recognition task. Fig. 3 provides a detailed depiction of how the gating network operates within a real-world LfO domain.

C. Action Recognition

In addition to recognizing the expert’s state, MVSA-Net also estimates the corresponding action at the current time step. As mentioned earlier, we have designed a network module comprising two time-distributed convolutional (TD-Conv) layers and two GRU layers to accomplish this. Additionally, a time-distributed max pooling layer is also incorporated for sub-sampling. These layers collect image features necessary for action recognition from multiple time steps ($t-4$, $t-3$, $t-2$, $t-1$). Each TD-Conv layer consists of 32 filters with a size of 3×3 and stride of 2×2 , while the pooling layer employs a filter of size 4×4 and stride of 3×3 . To further compose higher-level features and capture temporal changes in the image sequence, two convolutional GRU layers are employed. Each of these two GRU layers is equipped with 32 kernels sized at 3×3 and stride of 2×2 . Similar to state recognition, we apply batch normalization for action recognition. Since spatial information is also crucial to determine the correct action, we grab the corresponding extracted features of the last time step from the state recognition stream. Similar to the state recognition branch, the action recognition branch incorporates

a gating network and decision module to optimize recognition performance.

In MVSA-Net, Negative Log Likelihood [23] and Adam [18] are used as the loss and optimization functions, respectively. Section IV discusses MVSA-Net’s performance using gating networks and compares it with the baselines under different conditions.

IV. EXPERIMENTS

We demonstrate the generalizability of MVSA-Net’s architecture for LfO by evaluating in two tasks across different domains. One task involves the robotic automation of processing line tasks, while the other focuses on mobile robot patrolling. We will provide brief descriptions of these domains, followed by our experimentation procedures and results.

A. Domain Specifications

Robot integration into produce processing. In this domain, a robot is tasked with observing and learning how a human sorts an arbitrary number of onions: separating blemished onions from unblemished ones. The human expert picks up onions from the conveyance and meticulously inspects them. If an onion is recognized as blemished, it gets discarded into a bin positioned next to the conveyor belt. Conversely, if it is deemed unblemished, the expert returns it to the conveyance and proceeds to inspect the next onion until all onions are processed. In our setting, the robot utilizes three heterogeneous depth cameras with different viewpoints.

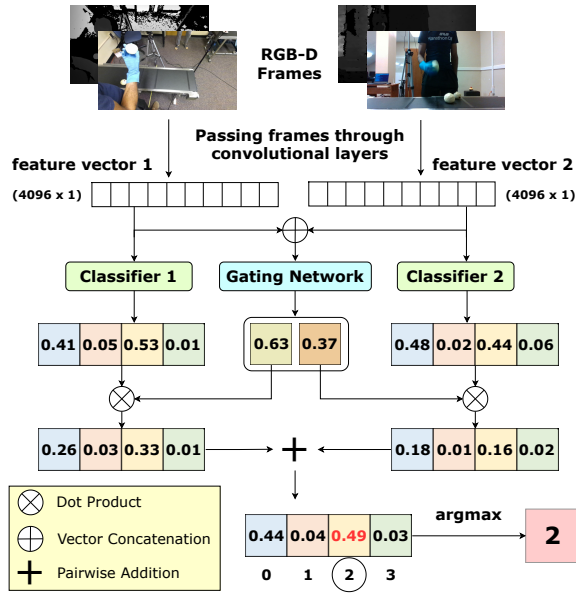


Fig. 3: A comprehensive example of how the gating network consolidates the results of two distinct classifiers into a solitary output value within the onion sorting domain for recognizing the onion location. The onion location comprises four possibilities, namely *at_home*, *on_conveyor*, *in_front*, and *at_bin*. Each of these states corresponds to an index ranging from 0 to 3, respectively. As depicted in the diagram, the gating network recognizes that classifier 1 provides more accurate predictions in these scenarios and assigns it a higher weight.

Specifically, we utilize an Intel RealSense D435i camera positioned in front of the expert, a Microsoft Kinect V2 camera on the side, and a Microsoft Azure camera above the expert’s shoulder. The latter camera offers a near-point-of-view perspective of the expert’s actions. Fig. 4 displays the views captured by these three cameras in this task.

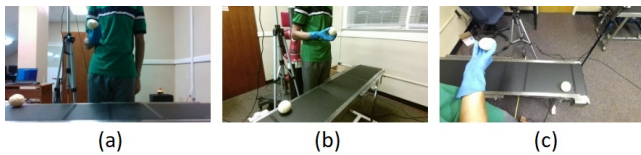


Fig. 4: Multiple viewpoints of onion sorting: (a) front, (b) side, and (c) top-down views.

The learner utilizes MVSA-Net to recognize both the states of the environment and the expert’s actions throughout the task. After obtaining trajectories from MVSA-Net, a robotic manipulator equipped with a gripper can learn the task parameters through imitation learning or inverse RL and subsequently execute the sorting. For the onion-sorting experiment, we collected a dataset consisting of 2,873 synchronized RGB-D frames.

The state can be adequately represented by three variables: the spatial location of the onion, the spatial location of the end-effector (hand), and whether the onion is blemished or not. Since the camera positions remain stationary, temporal information may not be necessary for state recognition,

and the current frame alone suffices. MVSA-Net employs convolutional and pooling layers for recognizing the onion and end-effector locations. Simultaneously, the onion’s status is determined using an auxiliary object detector (YOLOv5). This information is then fed into MVSA-Net’s decision module to create a comprehensive state representation. We segment the RGB frame into four exclusive spatial regions (*on_conveyor*, *at_home*, *in_front*, and *at_bin*), as shown in Fig. 5, to turn the end-effector and onion location recognition into a classification problem with a finite number of classes. Also, the status of each onion can be either *blemished*, *unblemished*, or *unknown*. Therefore, 48 different state classes (combinations of end-effector locations, onion locations, and onion status) are possible here. The action classes in this domain include *claim*, *inspect*, *place_in_bin*, and *place_on_conveyor*. Note that we assign one of the state classes and one of the action classes to each of the training frames. For instance, the ground truth state label for the frame shown in Fig. 5 is (*in_front*, *in_front*, *unblemished*) representing end-effector location, onion location, and onion status, respectively; and the action class is *inspect*.



Fig. 5: Pre-defined spatial regions for the onion and end-effector locations from the front-view camera. In this example, onion and end-effector locations are both in the *in_front* region. Furthermore, the onion status is *unblemished* and the action is *inspect*.

Multiple onions usually appear in a single frame. To focus YOLO’s blemish recognition on the onion currently under inspection, we establish a set of conditions to achieve the desired outcome. Prior to assessing these conditions, all onion detections are arranged in descending order based on their classification confidence. Subsequently, each candidate bounding box and its predicted label are taken into consideration. The conditions are defined within a decision module in the final step of MVSA-Net:

- If no onion is detected with classification confidence of 0.5 or higher, the status is marked as *unknown*.
- If the Euclidean distance between the onion and the end-effector is less than 40 pixels, the onion’s label is returned.
- Otherwise, the label of the closest onion to the end of the conveyor belt is chosen, and others are disregarded.

Lastly, we need to consolidate predictions from various viewpoints into a single prediction for the status of each onion. It’s important to note that a blemished onion may only exhibit the blemish from one viewpoint. Consequently, we establish

conditions in the decision module to determine the final label for the targeted onion: If all detections are *unknown*, the onion’s status remains *unknown*. However, if at least one viewpoint detects a blemish, then the status is classified as *blemished*; otherwise, it is categorized as *unblemished*. If all detections are *unknown*, then the onion’s status is *unknown*. If at least one viewpoint detects a blemish, then the status is *blemished*, otherwise, the status is *unblemished*.

Penetrating robotic patrolling. In this domain, an attacker (a TurtleBot2 with an RGB-D camera) observes the movement of two independent patrolling robots (also TurtleBots) from two vantage points. The attacker’s objective is to reach a predetermined location without being spotted by the patrolling robots, which have a limited field of view [6]. In this scenario, the attacker employs MVSA-Net to recognize the states and actions of the patrollers. The state parameters are the poses (X, Y , and the orientation θ) of the patrolling TurtleBots, with coordinates derived from a 2D map of a hallway (refer to Fig. 6) where the patrollers travel and the orientation is one of four directions, *north*, *south*, *east*, and *west*. The action classes here include *move_forward*, *turn_right*, *turn_left*, and *stop*. If YOLOv5 fails to detect the TurtleBot2, the network classifies this as *unknown* for all state and action parameters. We employ the same configuration as in prior applications of this domain [4], [27], with the exception that in our experiment, the attacker utilizes an auxiliary camera to gain an extra perspective of the environment.

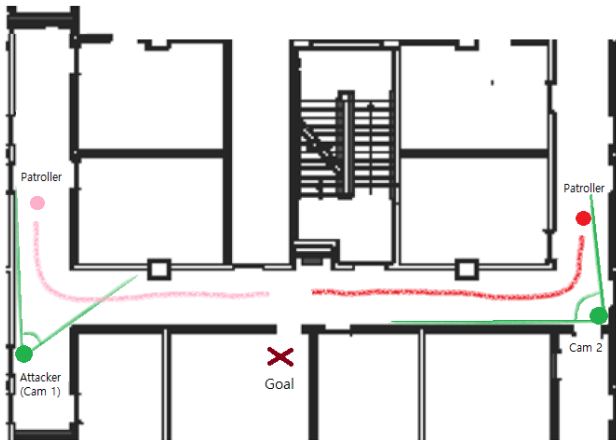


Fig. 6: The floor map in our patroller-attacker domain. The attacker is equipped with two Kinect V2 cameras (Cam 1 and Cam 2), each with a limited field of view shown in green. The initial position of the patrolling robots and the goal of the attacker is also depicted.

Note that in comparison to the previous domain, MVSA-Net recognizes the state-action pairs of multiple experts instead of a single expert, for which the masking filter is activated. Additionally, Cam 2 is positioned on the opposite side of the hallway to provide the attacker with a view of both the long and short hallways. Fig. 7 depicts the physical setup and the field of view of the two cameras used by the attacker. The dataset gathered in this domain comprises 5,110 synchronized RGB-D frames captured by each of the two attacker cameras, with a consistent frame rate of 10 FPS.



Fig. 7: Two different viewpoints of the attacker TurtleBot2. (a) primary view (Cam 1); (b) supplementary view (Cam 2).

B. Baselines

We assess MVSA-Net’s performance in comparison to three baseline methods:

- 1) SA-Net [27], which is a single-view state-action pair recognition method;
- 2) A two-stream VGG-Net [25] which is an action recognition pipeline; and
- 3) An ablation of MVSA-Net wherein we substitute the gating network with a single classifier and eliminate all other classifiers. The input is the set of aggregated features extracted from each viewpoint, similar to the input of the gating network. Onion status prediction is determined through majority voting in the multi-view baselines.

TABLE I: Mean classification accuracy (%) on the onion-sorting task. Note that ‘—’ denotes not applicable.

Method	Onion	End-effector	Onion	Action
	Location	Location	Status	
Single-view SA-Net (front view)	85.70±0.1	91.02±0.1	40.06±0.2	93.70±0.1
Single-view SA-Net (side view)	86.24±0.1	90.83±0.1	39.40±0.2	91.44±0.1
Single-view SA-Net (top-down view)	72.09±0.3	72.76±0.3	59.27±0.7	80.07±0.2
Two-Stream VGG-Net (front view)	—	—	—	80.92±0.1
Two-Stream VGG-Net (side view)	—	—	—	76.26±0.2
Two-Stream VGG-Net (top-down view)	—	—	—	69.51±0.2
Two-Stream VGG-Net (multi-view)	—	—	—	80.92±0.1
MVSA-Net without gating network	87.15±0.1	92.11±0.1	64.24±0.2	95.66±0.1
MVSA-Net	89.84±0.1	95.68±0.1	68.21±0.2	97.67±0.1

TABLE II: Evaluation on the patroller-attacker experiment.

Method	X	Y	θ	Action
Single-view SA-Net (Cam 1)	19.72±0.1	16.58±0.1	18.29±0.6	18.37±0.1
Single-view SA-Net (Cam 2)	59.87±0.3	67.04±0.3	64.60±0.5	65.93±0.2
Two-Stream VGG-Net (Cam 1)	—	—	—	14.18±0.4
Two-Stream VGG-Net (Cam 2)	—	—	—	52.95±0.9
Two-Stream VGG-Net (multi-view)	—	—	—	84.86±0.4
MVSA-Net without gating network	90.48±0.1	92.91±0.2	93.12±0.2	93.09±0.2
MVSA-Net	94.66±0.1	97.03±0.1	97.88±0.2	96.72±0.1

Formative Evaluation. In both domains, we assess classification accuracy through 5-fold cross-validation and compare MVSA-Net’s performance against the baseline methods. Table I shows that the single-view models perform poorly, particularly in detecting the onion status. MVSA-Net outperforms all single-view pipelines by a considerable margin in both state and action recognition. Thus, the multi-view setup is indeed significantly more robust than single views. MVSA-Net also achieves superior accuracy compared to the multi-view

ablation that does not use the gating networks, demonstrating the effectiveness of incorporating the gating network into the architecture. We present analogous performance comparisons in the patrolling domain in Table II, where Cam 2 clearly provides more informative results than Cam 1, and MVSA-Net effectively leverages both views.

Ablation and Robustness Study. We conduct ablation experiments to demonstrate the efficacy of the depth channel and the importance of the connections between the state and action networks. We also evaluate the robustness of MVSA-Net in scenarios where relatively high levels of noise occur due to unreliable sensing. For the robustness tests, we created two datasets: one containing noisy RGB images and the other containing overexposed images. These form one of the multiple streams from the camera. As shown in Tables III and IV, MVSA-Net successfully retrieves valuable information from the cameras that remain unaffected by noise or extreme brightness, maintaining its high performance in these realistic scenarios.

TABLE III: Performance of ablated MVSA-Net and under noisy input and bad lighting settings for the onion-sorting task. Note that adding noise completely distorts onion status prediction.

Method	Onion Location	End-effector Location	Onion Status	Action
Architecture Ablations				
MVSA-Net w/o connection between state & action networks	89.84±0.1	95.68±0.2	68.21±0.3	93.20±0.1
MVSA-Net w/o depth channel	83.96±0.7	87.90±0.9	68.21±1.0	89.78±0.7
Robustness to Noise				
SA-Net w/ noise (front view)	62.79±1.5	68.44±1.2	0.0±0.0	79.23±1.1
Multi-view ablation w/ noise	86.05±0.3	87.71±0.3	62.58±0.4	90.87±0.2
MVSA-Net w/ noise	88.70±0.2	89.69±0.3	65.23±0.3	92.97±0.2
Robustness to Bad Lighting				
SA-Net w/ bad lighting (front view)	84.17±0.1	89.20±0.2	31.79±1.5	90.51±0.2
MVSA-Net without gating network w/ bad lighting	86.36±0.1	90.02±0.2	68.02±0.2	92.88±0.2
MVSA-Net w/ bad lighting	89.04±0.1	90.70±0.1	68.02±0.2	92.88±0.2

TABLE IV: Ablation performance and under noisy streams for the Patrolling domain.

Method	X	Y	θ	Action
Architecture Ablations				
MVSA-Net w/o connection between state & action networks	94.66±0.2	97.03±0.3	97.88±0.2	91.72±0.3
MVSA-Net w/o depth channel	86.49±0.7	90.81±0.7	92.33±1.8	90.26±1.0
Robustness to Noise				
SA-Net w/ noise (Cam 1)	14.45±1.0	12.64±0.8	14.90±2.1	15.53±1.9
Multi-view ablation w/ noise	88.29±0.5	89.87±0.5	92.33±0.9	90.45±1.2
MVSA-Net w/ noise	90.36±0.5	92.83±0.3	95.13±0.9	93.08±0.9
Robustness to Bad Lighting				
SA-Net w/ bad lighting (Cam 1)	19.04±1.2	15.78±1.1	16.98±1.9	16.94±1.7
MVSA-Net without gating network w/ bad lighting	89.90±0.4	90.52±0.3	92.66±0.7	92.07±0.9
MVSA-Net w/ bad lighting	92.85±0.4	95.11±0.3	96.29±0.4	94.05±0.7

Evaluating MVSA-Net toward LfO. In order to assess the effectiveness of the state-action trajectories provided by MVSA-Net, we use these trajectories as input for the state-of-the-art inverse RL algorithm, MAP-BIRL [8]. In our evaluation, we employ a commonly adopted metric for

inverse RL called learned behavior accuracy (LBA). LBA compares the learned policy with the true expert policy to determine the quality of the learned policy. To achieve this, we conduct 10 independent trials of onion sorting yielding 10 trajectories each comprising 40 ± 5 steps of state-action pairs. Two different human subjects performed the sorting task (each performed 5 trials) to enhance the model’s robustness. *Utilizing the predictions provided by MVSA-Net resulted in an LBA of 97.9% as compared to 83.3% using the single-view SA-Net on the top-down view.* Therefore, MVSA-Net’s multi-view fusion generates state-action trajectories that result in significantly improved LfO performance compared to single-view trajectories. This improvement is attributed to its robustness in handling occlusion and inherent sensor noise. As such, we provide evidence that MVSA-Net can be directly applied in real-world robotic domains, leading to substantially improved outcomes (**please refer to the supplementary video for more details.**)

V. CHALLENGES AND FUTURE WORK

During the development of our pipeline, a few practical considerations came to light, though they are often just part of the typical development landscape. The future, meanwhile, holds promise for even more enhanced capabilities.

Challenges. Operating multiple cameras on a single system poses a significant demand for hardware. This necessitates robust and optimized hardware to ensure smooth and uninterrupted functioning. We solved this by distributing the process into multiple machines. Our model mandates that all cameras transmit their data concurrently. However, achieving this synchronicity is challenging. This is because of inevitable camera latencies and the varied processing speeds of heterogeneous camera systems, making simultaneous data transmission a formidable task. To handle this, we fix the capturing speed to 10 FPS to minimize the processing latency.

Future Work. Looking ahead, we aim to increase our system’s processing speed to 20 FPS or higher by decreasing the synchronization latency. Also, the current design recognizes actions based on a fixed number of consecutive frames. A promising direction would be to make the model more adaptive by first determining the duration of the action and subsequently recognizing the action. This can cater to actions that might not neatly fit within the fixed-frame window, offering more flexibility and accuracy. Additionally, we hope to make our system more adaptable to different camera positions between training and testing. This can be achieved by employing data augmentation techniques and providing more versatile training data. Another promising future extension would be to modify MVSA-Net’s architecture by replacing the classification network with a regression model, allowing for continuous state-action predictions.

In sum, while our current model stands as a significant contribution to the domain, there remains much room for growth and adaptation.

VI. CONCLUSIONS

We introduce MVSA-Net, a novel architecture that handles inputs from multiple viewpoints to articulate desiderata while learning a robust model. Tailored meticulously for dependable robotic systems, MVSA-Net improves upon single-view architectures by leveraging information from multiple viewpoints, enabling efficient inference with noisy input streams. While using multiple viewpoints is common in literature, our novelty lies in performing state and action recognition from various perspectives. The results show our approach surpasses baseline methods in prediction accuracy, potentially enabling more effective robot deployment in noisy environments. Future enhancements may focus on system speed, adaptive action recognition, camera flexibility, and continuous state-action predictions.

ACKNOWLEDGMENT

We thank Prasanth Suresh for providing the MAP-BIRL baseline for IRL evaluations and experimentation assistance. This work was enabled in part by NSF grant #IIS-1830421 and a Phase 1 grant from the GA Research Alliance to PD.

REFERENCES

- [1] S. Amirian, Z. Wang, T. R. Taha, and H. R. Arabnia. Dissection of deep learning with applications in image recognition. In *2018 International Conference on Computational Science and Computational Intelligence (CSCI)*, pages 1142–1148. IEEE, 2018.
- [2] B. D. Argall, S. Chernova, M. Veloso, and B. Browning. A survey of robot learning from demonstration. *Robotics and Autonomous Systems*, 57(5):469–483, 2009.
- [3] S. Arora and P. Doshi. A survey of inverse reinforcement learning: Challenges, methods and progress. *CoRR*, abs/1806.06877, 2019.
- [4] S. Arora, P. Doshi, and B. Banerjee. Online inverse reinforcement learning under occlusion. In *Proceedings of the 18th International Conference on Autonomous Agents and MultiAgent Systems*, pages 1170–1178, 2019.
- [5] E. Asali, F. Shenavarmasouleh, F. G. Mohammadi, P. S. Suresh, and H. R. Arabnia. Deepmsrf: A novel deep multimodal speaker recognition framework with feature selection. In *Advances in Computer Vision and Computational Biology*, pages 39–56. Springer, 2021.
- [6] K. Bogert and P. Doshi. Multi-robot inverse reinforcement learning under occlusion with interactions. In *International Conference on Autonomous Agents and Multi-Agent Systems*, pages 173–180, 2014.
- [7] K. Bogert and P. Doshi. A hierarchical bayesian process for inverse rl in partially-controlled environments. In *Proceedings of the 21st International Conference on Autonomous Agents and Multiagent Systems*, AAMAS '22, page 145–153, 2022.
- [8] J. Choi and K.-E. Kim. Map inference for bayesian inverse reinforcement learning. *Advances in Neural Information Processing Systems*, 24, 2011.
- [9] J. Chung, S. Ahn, and Y. Bengio. Gating networks. In *Advances in Neural Information Processing Systems*, pages 3473–3481, 2015.
- [10] G. Cortes and S. Doncieux. Using depth cameras for robot navigation. In *2012 IEEE/RSJ International Conference on Intelligent Robots and Systems*, pages 2489–2494. IEEE, 2012.
- [11] C. Fan, J. Zhu, J. Tan, and X. Liu. Robust human detection and tracking using rgb-d camera for mobile robots. In *2016 IEEE International Conference on Robotics and Biomimetics (ROBIO)*, pages 1716–1721. IEEE, 2016.
- [12] P. Gräve, A. Roennau, and S. Behnke. 3d object recognition and pose estimation with a depth camera for robotic bin picking. In *2014 IEEE International Conference on Robotics and Automation (ICRA)*, pages 2338–2344. IEEE, 2014.
- [13] K. He, X. Zhang, S. Ren, and J. Sun. Deep residual learning for image recognition. In *IEEE Conference on Computer Vision and Pattern Recognition*, pages 770–778, 2016.
- [14] S. Hochreiter and J. Schmidhuber. Long short-term memory. *Neural Computation*, 9(8):1735–1780, 1997.
- [15] S. Ioffe and C. Szegedy. Batch normalization: Accelerating deep network training by reducing internal covariate shift. In *International conference on machine learning*, pages 448–456. PMLR, 2015.
- [16] M. M. Islam, S. Nooruddin, F. Karray, and G. Muhammad. Human activity recognition using tools of convolutional neural networks: A state of the art review, data sets, challenges, and future prospects. *Computers in Biology and Medicine*, page 106060, 2022.
- [17] H. Kasaei, S. Luo, R. Sasso, and M. Kasaei. Simultaneous multi-view object recognition and grasping in open-ended domains. *arXiv preprint arXiv:2106.01866*, 2021.
- [18] D. P. Kingma and J. Ba. Adam: A method for stochastic optimization. In *International Conference on Learning Representations*, 2015.
- [19] Z. Liu, Z. Yin, and Y. Wu. Mlrmv: Multi-layer representation for multi-view action recognition. *Image and Vision Computing*, 116:104333, 2021.
- [20] Y. Lu and Y. Shu. Custom object detection via multi-camera self-supervised learning. *arXiv preprint arXiv:2102.03442*, 2021.
- [21] H. Ma, W. Li, X. Zhang, S. Gao, and S. Lu. Attmsense: Multi-level attention mechanism for multimodal human activity recognition. In *IJCAI*, pages 3109–3115, 2019.
- [22] R. Martín-Nieto, Á. García-Martín, J. M. Martínez, and J. C. San-Miguel. Enhancing multi-camera people detection by online automatic parametrization using detection transfer and self-correlation maximization. *Sensors*, 18(12):4385, 2018.
- [23] T.-T. Nguyen, M. H. Khani, and O. A. von Lilienfeld. Negative log-likelihood regularization. *Journal of Chemical Physics*, 152(23):234106, 2020.
- [24] J. Redmon, S. Divvala, R. Girshick, and A. Farhadi. You only look once: Unified, real-time object detection. In *Proceedings of the IEEE conference on computer vision and pattern recognition*, pages 779–788, 2016.
- [25] F. Rezazadegan, S. Shirazi, B. Upcroft, and M. Milford. Action recognition: From static datasets to moving robots. In *IEEE International Conference on Robotics and Automation (ICRA)*, pages 3185–3191, 2017.
- [26] P. W. Shin, J. Sampson, and V. Narayanan. Context-aware collaborative object recognition for distributed multi camera time series data. In *Proceedings of the Tenth International Symposium on Information and Communication Technology*, pages 154–161, 2019.
- [27] N. Soans, E. Asali, Y. Hong, and P. Doshi. Sa-net: Robust state-action recognition for learning from observations. In *2020 IEEE International Conference on Robotics and Automation (ICRA)*, pages 2153–2159. IEEE, 2020.
- [28] B. Strbac, M. Gostovic, Z. Lukac, and D. Samardzija. Yolo multi-camera object detection and distance estimation. In *2020 Zooming Innovation in Consumer Technologies Conference (ZINC)*, pages 26–30. IEEE, 2020.
- [29] P. S. Suresh and P. Doshi. Marginal MAP estimation for inverse RL under occlusion with observer noise. In *Proceedings of the Thirty-Eighth Conference on Uncertainty in Artificial Intelligence*, pages 1907–1916, 2022.
- [30] A. Ullah, J. Ahmad, K. Muhammad, M. Sajjad, and S. W. Baik. Action recognition in video sequences using deep bi-directional lstm with cnn features. *IEEE Access*, 6:1155–1166, 2017.
- [31] S. Vyas, Y. S. Rawat, and M. Shah. Multi-view action recognition using cross-view video prediction. In *European Conference on Computer Vision*, pages 427–444. Springer, 2020.
- [32] D. Wang, W. Ouyang, W. Li, and D. Xu. Dividing and aggregating network for multi-view action recognition. In *Proceedings of the European Conference on Computer Vision (ECCV)*, pages 451–467, 2018.
- [33] P. Wang, W. Li, Z. Gao, Y. Zhang, C. Tang, and P. Ogunbona. Scene flow to action map: A new representation for RGB-D based action recognition with convolutional neural networks. In *IEEE Conference on Computer Vision and Pattern Recognition (CVPR)*, pages 416–425, 2017.
- [34] X. Wang, L. Gao, J. Song, and H. Shen. Beyond frame-level cnn: saliency-aware 3-d cnn with lstm for video action recognition. *IEEE Signal Processing Letters*, 24(4):510–514, 2016.
- [35] J. Yue-Hei Ng, M. Hausknecht, S. Vijayanarasimhan, O. Vinyals, R. Monga, and G. Toderici. Beyond short snippets: Deep networks for video classification. In *Proceedings of the IEEE Conference on Computer Vision and Pattern Recognition*, pages 4694–4702, 2015.